## "Non-stick" Membranes Prepared by Facile Surface Fluorination for Water Purification

Thien Tran, <sup>1</sup> Yi-Chen Tu, <sup>1</sup> Stephanie Hall-Laureano, <sup>2</sup> Chen Lin, <sup>1</sup> Mohamed Kawy, <sup>1</sup> and Haiqing Lin<sup>1,\*</sup>

<sup>1</sup> Department of Chemical and Biological Engineering, University at Buffalo, The State
University of New York, Buffalo, NY 14260, USA.

<sup>2</sup> University of Puerto Rico at Mayaguez, Mayaguez, 00682, Puerto Rico

<sup>\*</sup>Corresponding author. Tel: +1-716-645-1856, Email: haiqingl@buffalo.edu (H. Lin)

**ABSTRACT** 

Polymeric membranes for water purification are faced with fouling by the aggregation of

contaminants on the surface, decreasing water permeance. Herein, we demonstrate facile

fluorination of ultrafiltration (UF) membranes by directly coating a "non-stick" amorphous

perfluoropolymer of Teflon<sup>TM</sup> AF1600 achieving optimally low surface energy with excellent

antifouling properties, while retaining surface pore structures and thus high water permeance. At

the Teflon AF1600 concentration of 200 ppm, the derived fluorinated layer has a thickness less

than 5 nm and shows an unexpected surface energy of 24 mN/m, very close to that with the

minimal biological fouling on the Baier's curve. When challenged with 0.5 g/L bovine serum

albumin solution in a constant-flux crossflow system, the fluorinated polyacrylonitrile (PAN) UF

membrane showed 54% lower fouling rate than the pristine one at a water flux of 60 liter/m<sup>2</sup> h.

This approach enables flexible control of the degree of fluorination and surface energy and can be

easily implemented in current membrane manufacturing processes.

**KEYWORDS:** 

Antifouling;

surface fluorination;

membranes;

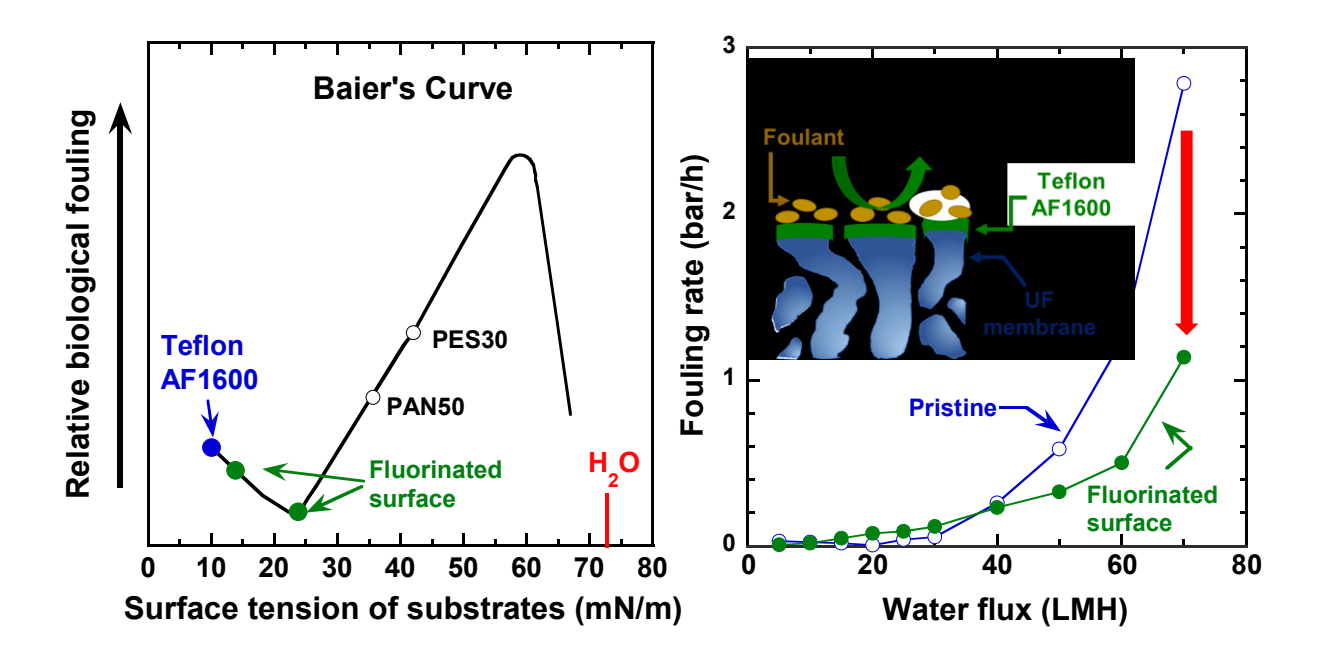
water p

purification;

perfluoropolymers

2

# **Table of Contents (TOC) Graphic**



#### 1. INTRODUCTION

Membrane technology has been widely practiced for water purification and wastewater treatment because of its high energy-efficiency and small footprint. <sup>1-3</sup> Membranes can permeate water and reject contaminants larger than their pore sizes, such as organic matters and suspended solids. However, as the water flows to the membrane surface and permeates through the membrane, these contaminants can accumulate on the membrane surface, creating additional transport resistance and decreasing water flux. An effective approach to mitigate the fouling is to minimize favorable interactions between the foulants and membrane surface. <sup>4-7</sup> Conventional approaches are to improve surface hydrophilicity by coating or grafting with hydrophilic materials such as poly(ethylene glycol) (PEG), <sup>8-10</sup> polydopamine (PDA), <sup>11, 12</sup> and zwitterionic materials. <sup>13-18</sup> These hydrophilic materials form a hydration layer on the membrane surface, which prevents favorable interactions between the surface and foulants. However, due to the hydrophilic nature of these materials, their long-term stability for underwater operation often presents a challenge.

Perfluoropolymers exhibit good underwater stability and non-stick nature with low foulant adsorption derived from their low surface energy.<sup>5, 6, 19</sup> For example, glass substrates coated with polyperfluoroacrylate exhibited surface energy of less than 13 mN/m and reduced bacterial adsorption.<sup>20</sup> Membrane surface has also been fluorinated to improve antifouling properties, and the shearing force derived from the feed flow can further remove the foulants off the membrane surface. For example, nanofiltration (NF) membrane was fluorinated by acylation reaction with fluorinated polyamines, which decreased the critical surface energy from 60 mN/m to 44 mN/m and increased the flux recovery to 98.5% when challenged with model protein solutions.<sup>21</sup> Reverse osmosis (RO) membrane was fluorinated via chemical vapor deposition (CVD) of an amphiphilic copolymer containing perfluorodecyl acrylate and hydrophilic hydroxyethyl methacrylate,

decreasing cell attachment.<sup>22</sup> Polyacrylonitrile (PAN) ultrafiltration (UF) membranes were hydrolyzed and then grafted with perfluoroalkyl groups, which showed a flux recovery ratio up to 99%.<sup>23</sup> However, these fluorination methods often involve complex chemistry, and it is very difficult to obtain low surface energy and a thin fluorinated layer without significant transport resistance simultaneously. In addition, for the UF membranes, the fluorinated layer cannot block the pores, which, otherwise, would dramatically decrease the water permeance.

Herein, we demonstrate, for the first time, facile fluorination of the UF membrane surface by directly coating a solution-processable perfluoropolymer of Teflon<sup>TM</sup> AF1600 to achieve nonstick properties while retaining high water permeance. Teflon AF1600 is amorphous consisting of perfluoro(2,2-dimethyl-1,2-dioxole) (PDD) and tetrafluoroethylene (TFE) and has a low attachment of cells.<sup>24</sup> Teflon AF1600 has excellent thin-film-forming properties and can form a dense selective layer of <50 nm on the UF membranes for gas separation, though the mechanism for such good thin film stability is not clear. 25, 26 By contrast, this study will show that when the coating solution is very dilute (<1000 ppm), Teflon AF1600 only deposits on the solid portion of the surface without covering the pores, retaining high water permeance. Specifically, two series of UF membranes of polyethersulfone (PES) and PAN with different molecular weight cutoffs (MWCO) were coated with solutions containing 50 – 1000 ppm Teflon AF1600. The effect of the fluorination on the membrane surface was thoroughly characterized using Fourier transform infrared (FTIR) spectroscopy, scanning electron microscopy (SEM), and a goniometer for contact angles. The use of the dilute solutions and resulted thin coatings (< 10 nm) would also make it economically viable for using these expensive perfluoropolymers. The improved antifouling properties on the fluorinated membrane surface are demonstrated by static adsorption test of a

model protein (bovine serum albumin or BSA) and water permeance measurement of BSA solutions using dead-end filtration systems and a constant-flux crossflow system.

#### 2. EXPERIMENTAL SECTION

Materials. Commercial PES UF membranes with various MWCOs were purchased from Synder® Filtration (Vacaville, CA). PAN50 was supplied by Sepro Membrane, Inc (Oceanside, CA). Teflon AF1600 was purchased from Chemours Company (Wilmington, DE). Ethoxynonafluorobutane (Novec 7200<sup>TM</sup>) was obtained from the 3M Company (Maplewood, MN). PEGs with various molecular weights, BSA, and PBS were obtained from Sigma-Aldrich (St. Louis, MO). BCA protein assay kit was supplied by BioVision (Milpitas, CA). Glycerol (≥99.7%) and IPA were purchased from VWR International (Radnor, PA). Diiodomethane (99%) was supplied by Alfa Aesar (Haverhill, MA). Cylinders of ultrahigh purity N₂ were supplied by Airgas (Radnor, PA).

Surface fluorination and characterization. Teflon AF1600 was dissolved in Novec 7200 with concentrations ranging from 100 ppm to 5000 ppm. The solution was coated on the membrane surface using an automatic draw machine (DP-8301, The Paul N. Gardner Company, Pompano Beach, FL). After the coating, the membrane was quickly dried using a heat gun. <sup>25,26</sup> The modified membranes were subsequently soaked in an isopropyl alcohol bath for 2 h then transferred to a DI water bath for at least 24h before any characterizations.

To determine the thickness of the coated layer, the solutions were directly coated onto silicon wafers (University Wafer, Inc., Boston, MA). After drying, the film thickness was determined using an F-20 thin-film analyzer (Filmetrics, Inc., San Diego, CA).<sup>25, 26</sup>

Surface chemistry of the modified membranes was characterized by attenuated-total-reflection FTIR (ATR-FTIR) spectroscopy (Vertex 70, Billerica, MA). 100 scans were conducted with wavenumbers from 600 to 4000 cm<sup>-1</sup> at a resolution of 2 cm<sup>-1</sup>. Surface hydrophilicity was determined using a goniometer (model 190, Rame-Hart Instrument Co., Succasunna, NJ) via the sessile drop method using liquid droplets of 2 μL. Five different locations of the membrane surface were measured to obtain an average value. Membrane surface morphology was characterized using a field emission SEM (Hitachi SU70, Tokyo, Japan). The samples were sputtered with gold nanoparticles before the observation.

The surface tension of the membrane can be related to the contact angle ( $\theta$ ) between a probing liquid droplet and the surface via the Owens-Wendt equation:<sup>27-29</sup>

$$\gamma_L(1+\cos\theta) = 2(\gamma_L^D \gamma_M^D)^{1/2} + 2(\gamma_L^P \gamma_M^P)^{1/2} \tag{1}$$

where  $\gamma_L^D$  and  $\gamma_L^P$  are the dispersive and polar components of the liquid surface tension, respectively, and  $\gamma_M^D$  and  $\gamma_M^P$  are the dispersive and polar components of the membrane surface tension, respectively. By determining the  $\theta$  values of three different probing liquids, diiodomethane (non-polar), water (polar), and glycerol (polar), the  $\gamma_M^D$  and  $\gamma_M^P$  can be calculated.<sup>30</sup> The surface tension of membrane or water,  $\gamma_L$  (mN/m), can be described as follow:<sup>27</sup>

$$\gamma_i = \gamma_i^D + \gamma_i^P \tag{2}$$

where  $\gamma_i^D$  represents van der Waals interactions, and  $\gamma_i^P$  refers to Coulombic interactions between dipoles (e.g., hydrogen bonds).<sup>27</sup>

The adsorption of BSA on the membrane surface was quantified using BCA protein assay. A membrane coupon ( $\approx$  3.75 cm in diameter) was first clamped in a cell, and the active membrane surface ( $\approx$  5 cm<sup>2</sup>) was equilibrated with 3 mL PBS buffer (pH = 7.4) for 30 min. Second, the PBS buffer was replaced with 1 g/L BSA solution (3 mL), and the membrane was incubated at  $\approx$  22 °C

for 2 h. Third, the membrane surface was washed with 10 mL PBS buffer to remove any loosely bound BSA. 2 mL BCA-reagent solution prepared following a protocol provided by the manufacturer was pipetted into the cell, and the sample was incubated at  $\approx$  22 °C for 2 h. Finally, the absorbance of the solution at 562 nm was measured using a UV-Vis spectrophotometer (VSP-UV, Vernier Software and Technology, Beaverton, OR). The amount of the protein on the surface was calculated using a predetermined calibration curve.

Characterization of water permeance. Pure-water permeance  $(A_W)$  was determined using dead-end filtration cells.<sup>31, 32</sup> The membranes were mounted in the cells and kept in DI water for at least 24 h before the measurement. The water permeance  $(A_W)$  can be calculated using the equation below:

$$A_W = \frac{J_W}{\Delta p} = \frac{V}{t\Delta p A_m} \tag{3}$$

where  $\Delta p$  (bar) is the transmembrane pressure (TMP),  $A_m$  is the active membrane area (m<sup>2</sup>), and V is the volume of water permeated (L) over t (h).

The MWCO of the modified membranes was determined by measuring the rejection of PEGs (Mn = 2, 4, 10, 20, and 35 kDa) using dead-end filtration cells. <sup>12</sup> The PEG rejection (R) can be calculated from equation 4:

$$R = \left(1 - \frac{C_P}{C_F}\right) \times 100\% \tag{4}$$

where  $C_F$  and  $C_P$  are the total organic carbon (TOC) concentration in the feed and the permeate, respectively. The TOC content was determined using a TOC-LCPH analyzer (Shimadzu Scientific Instruments, Inc., Columbia, MD).

The antifouling properties of the membranes were characterized using two methods. The first method was to determine the pure-water flux before and after exposure to 1 g/L BSA solution

using dead-end filtration cells.<sup>33</sup> The second method was to use a custom-built constant-flux crossflow system (as shown in Fig. S2).<sup>34</sup> The membranes were tested at pre-set fluxes while the  $\Delta p$  (or TMP) values are monitored. During the fouling process, the feed pressure was kept at constant while the permeate pressure was decreased to retain the targeted water flux.<sup>12</sup>

#### 3. RESULTS AND DISCUSSION

#### 3.1. Surface fluorination and characterization

Figure 1a displays a schematic of the facile fluorination of the membrane surface by directly coating dilute solutions containing Teflon AF1600. The thin Teflon AF1600 layer covers the solid portion of the surface without significantly blocking the pores, thus leading to the fluorinated surface and retained water permeance. The modified membranes are denoted as PESx-y or PANx-y, where x is the MWCO of the membrane (kDa), and y is the concentration of Teflon AF1600 in the coating solutions (ppm).

Baier and coworkers performed an exhaustive review of biological fouling properties on various surfaces (cf. Figure 1b) and found that the surface exhibits the least fouling when the  $\gamma_M$  is close to the water  $\gamma_L^P$  (21.8 mN/m) and the most fouling when the  $\gamma_M$  is close to the water  $\gamma_L^P$  (51.0 mN/m), though the mechanism is not well understood.<sup>27, 35, 36</sup> As the surface energy approaches that of water ( $\gamma_L = 72.8$  mN/m), a hydration layer forms on the surface, resulting in a decrease in biofouling. In contrast to conventional approaches of increasing hydrophilicity to improving antifouling properties, this study aims to tailor the degree of fluorination to achieve the  $\gamma_M$  values close to 21.8 mN/m.

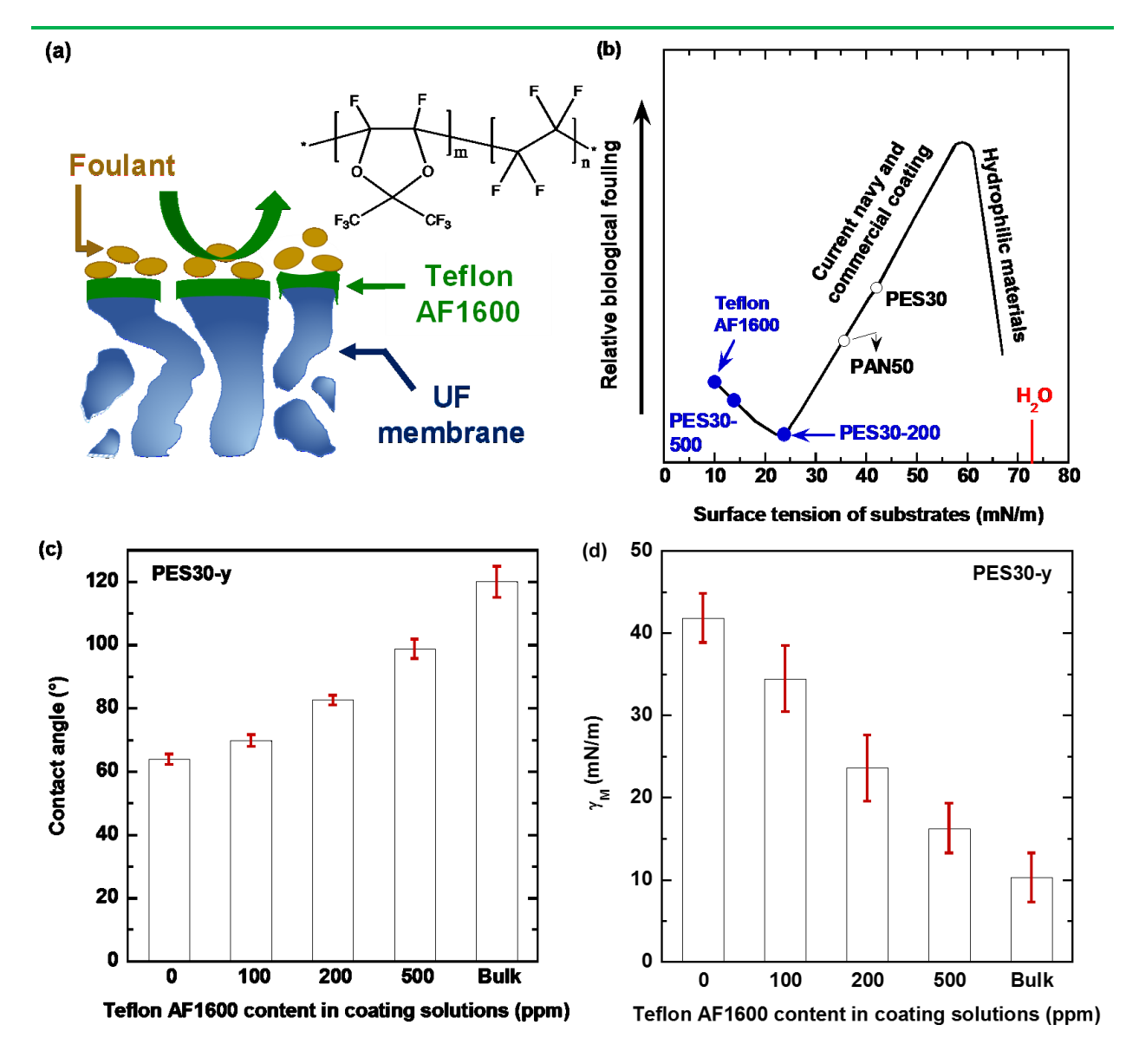


Figure 1. (a) Schematic of fluorination of the membrane surface by directly coating with dilute Teflon AF1600 solutions. (b) Baier's curve of relative biological fouling as a function of surface tension of substrates.<sup>35, 36</sup> The Y-axis is only for qualitative comparison, and the data points are the predicted biological fouling corresponding to the measured surface tension. Effect of Teflon AF1600 content in the coating solutions on (c) the water contact angle and (d) surface tension of the membranes ( $\gamma_M$ ) at  $\approx$ 22 °C. The error bar is the standard deviation of five measurements.

Figure 1c validates the success of the surface fluorination by the contact angle measurement. PES30 has a water contact angle ( $\theta$ ) of 64°, and PES30-500 has the  $\theta$  value of 99° (approaching 119° for the bulk polymer). As the concentration of Teflon AF1600 in the coating solutions (y values) increases, the membrane surface becomes more hydrophobic, and the degree of fluorination increases due to the increase of the thickness of the Teflon AF1600 layer.

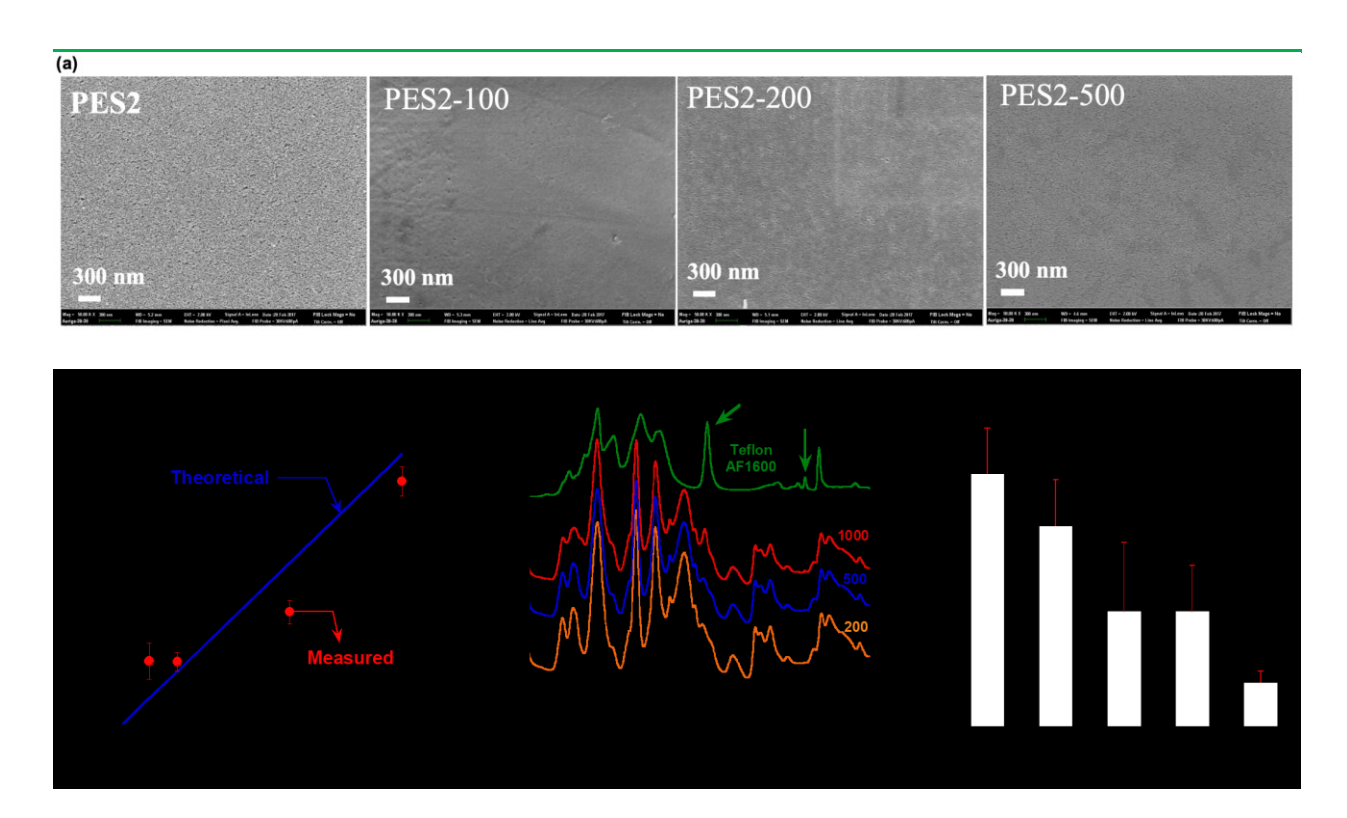
Figure 1d shows that the  $\gamma_M$  value decreases from 42 mN/m for the PES30 to 16 mN/m for PES30-500, approaching the surface tension of the bulk Teflon AF1600 (10 mN/m). Interestingly, the PES30-200 membrane exhibits a  $\gamma_M$  value of  $\approx$  24 mN/m, very close to  $\gamma_L^D$  for the lowest biofouling on the Baier's curve. These results suggest that the coating layer may exhibit unique antifouling properties more superior than the bulk polymer when coupled with the substrate.

Figure 2a compares the SEM images of the pristine and modified membrane surface. Increasing the *y* values decreases the pore size and makes the surface smoother. When the Teflon AF1600 concentration in the coating solution is 1000 ppm or higher, it is difficult to observe the pores on the surface except for some wrinkles formed by the gold coating for the SEM characterization (as shown in Figure S1 in the Supporting Information or SI).

Figure 2b presents the effect of the y values on the thickness of the resulting coating layer on silicon wafers. The theoretical thickness was estimated based on the liquid film thickness and the y values. If the Teflon AF1600 concentration is less than 500 ppm, freestanding thin films cannot be obtained, and thus, the film thickness cannot be determined. At higher concentrations, the measured thickness (7 - 28 nm) is consistent with the theoretical values and increases with increasing the y values.

Figure 2c compares the FTIR spectra of the pristine and fluorinated membranes. Teflon AF1600 exhibits a characteristic peak of  $\approx$ 960 cm<sup>-1</sup> for -CF<sub>3</sub> vibration and  $\approx$ 750 cm<sup>-1</sup> for the

amorphous character.<sup>37</sup> As the y values increase, the intensity of the peak at  $\approx$ 960 cm<sup>-1</sup> increases, and the peak shifts toward the right presumably due to the overlapping with the peak at 980 cm<sup>-1</sup> in the pristine PES30. Additionally, the peak at  $\approx$ 750 cm<sup>-1</sup> is noticeable only for the PES30-1000 and bulk polymer because this signal is weak, and the coating layer (< 10 nm, cf. Figure 2b) is too thin in PES30-200 and PES30-500.



**Figure 2.** (a) Surface SEM images of PES2, PES2-100, PES2-200, and PES2-500. (b) Effect of the coating solution composition on the thickness of the coating layers on silicon wafers. (c) FTIR spectra of the PES30 and the fluorinated ones. (d) Effect of the coating solution composition on protein (i.e., BSA) adsorption at  $\approx 22$  °C. The error bar is the standard deviation of 5 different measurements.

Figure 2d shows that the fluorination of the membrane surface decreases the adsorption of BSA, a model foulant to characterize antifouling properties. For example, PES30 shows the BSA adsorption of 11  $\mu$ g/cm<sup>2</sup>, much higher than PES30-200 (5  $\mu$ g/cm<sup>2</sup>) and PES30-1000 (2  $\mu$ g/cm<sup>2</sup>). This result validates that the facile fluorination process can lower the membrane surface tension and improve the antifouling properties of the membranes.<sup>35</sup>

## 3.2. Effect of the surface fluorination on water permeance of UF membranes

Figure 3a presents the effect of the surface fluorination on the pure water permeance of the UF membranes. Increasing the Teflon AF 1600 concentration in the coating solutions from 0 to 5000 ppm drastically reduces the water permeance from 81 liter/m² h bar (LMH/bar) to 0.8 LMH/bar, due to the decreased pore size (cf. Figure 2a) and increased hydrophobicity (cf. Figure 1b). The decrease in the surface pore size can be further confirmed by the MWCO measurement using PEG as a probe, as shown in Figure 3b. The MWCO is defined as the PEG molecular weight with a rejection of 90% in the membranes. The nominal pore size of the membrane equals to the Stoke-radius of the PEG with the 90% rejection, which is estimated using equation 5:<sup>12</sup>

$$a = 16.73 \times 10^{-3} M_W^{0.557} \tag{5}$$

where a is the Stoke-radius (nm), and Mw is the molecular weight of PEG (g/mol).

PES30-200 has the nominal pore size  $(5.6 \pm 0.1 \text{ nm})$  the same as the pristine PES30, and it exhibits higher rejection for PEG-4k and PEG-2k than PES-30, suggesting that small pores have been covered or restricted after coating with the solution containing 200 ppm Teflon AF1600. An additional increase of the Teflon AF1600 concentration in the coating solutions reduces the membrane nominal pore size to 2.8 nm for PES30-350 and less than 2 nm for PES30-1000.

Nevertheless, these MWCO values indicate that the surface pores are not completely covered by the coating, confirming the schematic shown in Figure 1a.

The stability of the perfluoropolymer coating was verified by measuring the water permeance of the modified membranes kept in the water bath for up to 2 weeks. The water permeance remains almost the same after the exposure to water, indicating the stability of the Teflon AF1600 coating, which is also consistent with the fact that the perfluoropolymers are stable underwater.<sup>20, 38</sup>

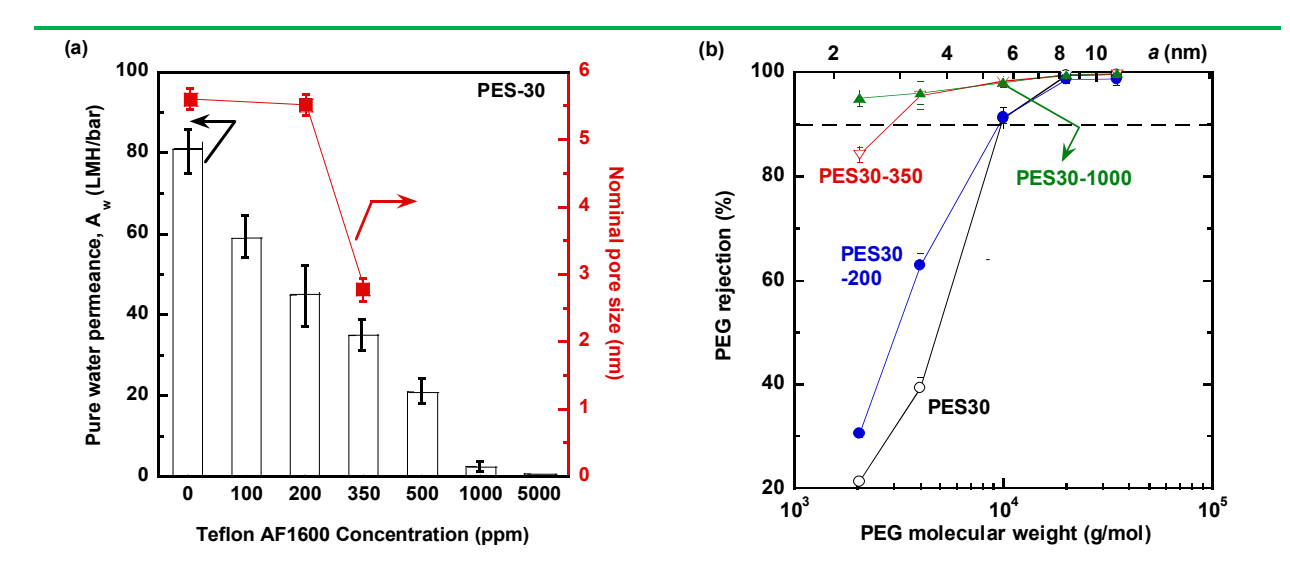


**Figure 3.** (a) Pure water permeance and the nominal pore size of the membranes, and (b) PEG rejection of the pristine and modified PES30 as a function of the y values. The error bar for water permeance and nominal pore size is the standard deviation of three membrane samples. Permeation tests were performed using dead-end filtration systems at 3.1 bar and  $\approx 22^{\circ}$ C

### 3.3. Antifouling properties of the fluorinated membranes

Figure 4 displays the antifouling properties of the membranes evaluated using dead-end filtration systems with BSA as the model foulant. The membranes were first tested with DI water

(with an initial water flux of  $J_{W,\theta}$ ) and then challenged with the 1 g/L BSA in phosphate buffer saline (PBS) solution (with the water flux of  $J_W$ ). After that, the cell was filled with 50 mL DI water and stirred for 2 min at 700 rpm. The solution was then discarded, and the process was repeated to clean the membrane and cell. After the cleaning, the pure water permeance ( $J_{W,l}$ ) was re-measured before testing with the BSA solution again. Figure 4a compares the relative water flux (i.e.,  $J_W/J_{W,\theta}$ ) in the PES30 and PES30-200 as a function of the permeate volume, instead of the time because the PES30-200 exhibits lower  $J_{W,\theta}$  value than PES30. The PES30-200 exhibits a relative water flux of  $\approx 0.72$ , which is higher than that of the PES30 ( $\approx 0.55$ ), suggesting the improved antifouling performance for the fluorinated membrane. After exposure to the BSA solution, the pure water flux does not fully recover due to the irreversible fouling (such as internal fouling). Similar behavior can also be observed for the PES30-350 with the  $J_W/J_{W,\theta}$  value of 0.75, as shown in Figure 4b. These results suggest that surface fluorination has essentially no impact on the internal fouling.

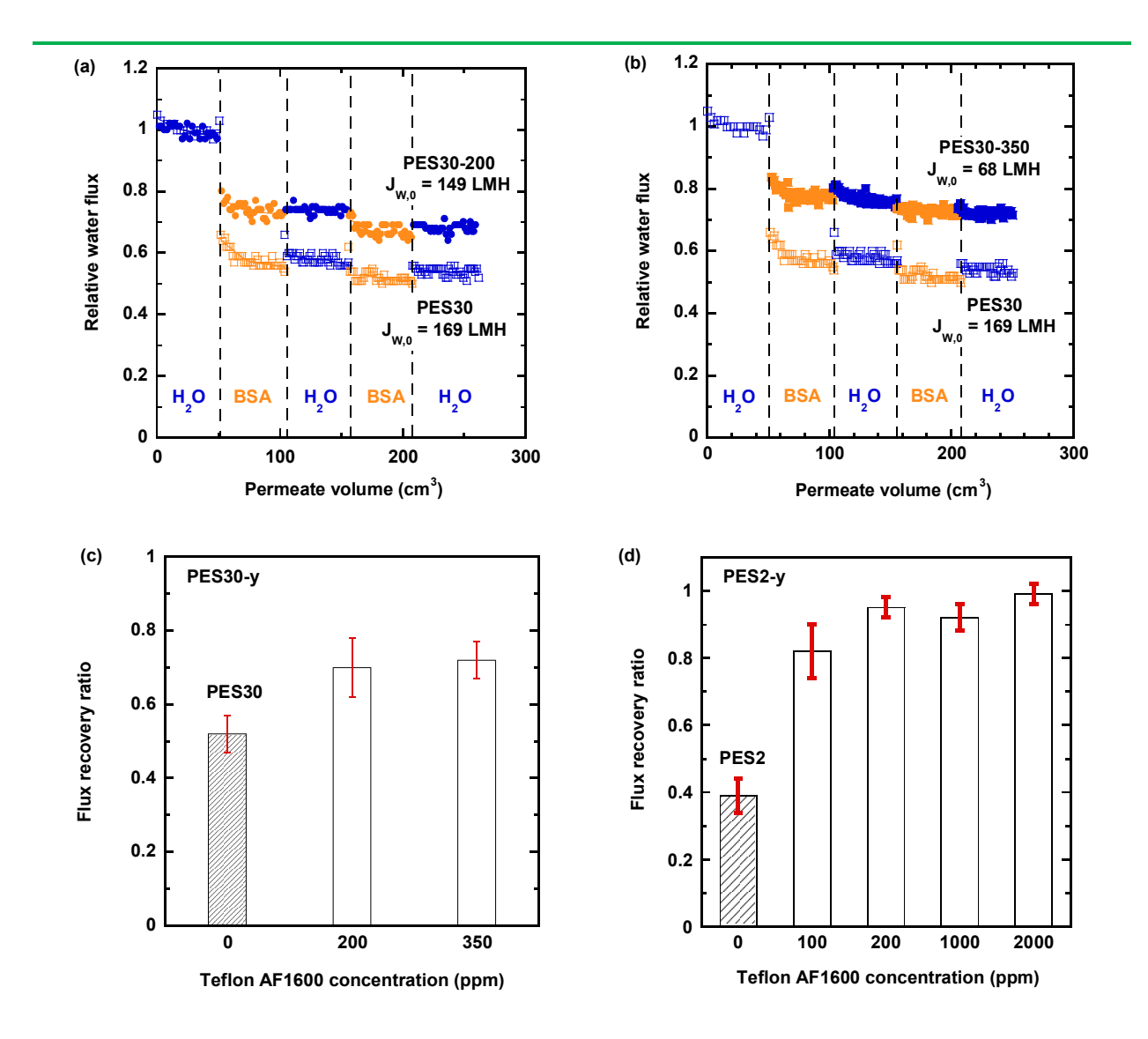


**Figure 4.** Relative water flux vs. the volume of the permeated water in (a) PES30-200 and (b) PES30-350 (filled symbols) in comparison with PES30 (open symbols). Effect of the fluorination on the flux recovery ratio for (c) PES30 and (d) PES2. Water flux was determined using dead-end filtration systems with pure water or 1 g/L BSA solutions at 3.1 bar and  $\approx$ 22 °C.

Figures 4c and 4d illustrate the effect of surface fluorination on the flux recovery ratio (FRR, defined as  $J_{W,1}/J_{W,0}$ ) of the PES30 and PES2 membranes, respectively. Interestingly, the PES2-100 shows a remarkable FRR value of 80%, which is twice the value of the PES2 ( $\approx$ 40%).

Further increase of the y values results in FRR values greater than 90%. These results are consistent with the BSA adsorption experiments, confirming that the low surface free energy of the Teflon AF1600 coating leads to unfavorable interactions with BSA.<sup>39</sup> Additionally, the surface fluorination improves antifouling properties more significantly for PES2 than PES30 because the larger pores in the PES30 may cause more significant irreversible fouling. For example, the FRR value is 0.92 for PES2-200 (with  $A_{W,0}$  of  $25 \pm 5$  LMH/bar), which is higher than that (0.70) for PES30-200 (with  $A_{W,0}$  of  $45 \pm 8$  LMH/bar).

Industrial membranes are often operated with constant flux below their threshold flux ( $J_{TH}$ , defined as the flux above which the fouling rate increases rapidly with increasing the water flux) to achieve stable productivity. <sup>12, 34, 40, 41</sup> Figure 5a provides an example of the flux stepping method to determine the  $J_{TH}$  values using a constant-flux crossflow system (cf. Figure S2). In contrast to dead-end filtration systems with constant TMP, the constant-flux system operates with a constant flux by varying the TMP values. In this study, the membranes were challenged with 0.5 g/L BSA solution, and the permeate flux was increased from 0 to 30 LMH (or 100 LMH) at an increment of 5 LMH until the TMP surpassed 2.1 bar. The duration of each step was 10 min.

As shown in Figure 5a, the TMP of PES30-200 remains constant at fluxes below 40 LMH, suggesting that fouling is insignificant at these low fluxes. However, at the permeate fluxes of 40 LMH and above, the TMP starts to increase, and the increasing rate becomes more rapid with increasing the flux. The  $J_{TH}$  can be determined by calculating the arithmetic average of the TMP at each flux and then plotting as a function of flux, as shown in Figure 5b.<sup>42, 43</sup> Two trends of the average TMP versus water flux can be observed, which can be fitted with linear lines. The intersection is defined as the  $J_{TH}$ .<sup>12, 40, 44</sup> PES30-200 shows a lower  $J_{TH}$  value (40 LMH) than the pristine PES30 (46 LMH) because of the lower water permeance (i.e., 49±5 LMH/bar vs. 80±6

LMH/bar) and thus smaller pores on the surface.<sup>45</sup> Additionally, PES30-200 shows higher rejection for PEG less than 10 kDa (cf. Figure 3b) than PES30, indicating that the small pores may be further narrowed by the surface coating, accelerating fouling and decreasing the  $J_{TH}$ .<sup>45</sup>

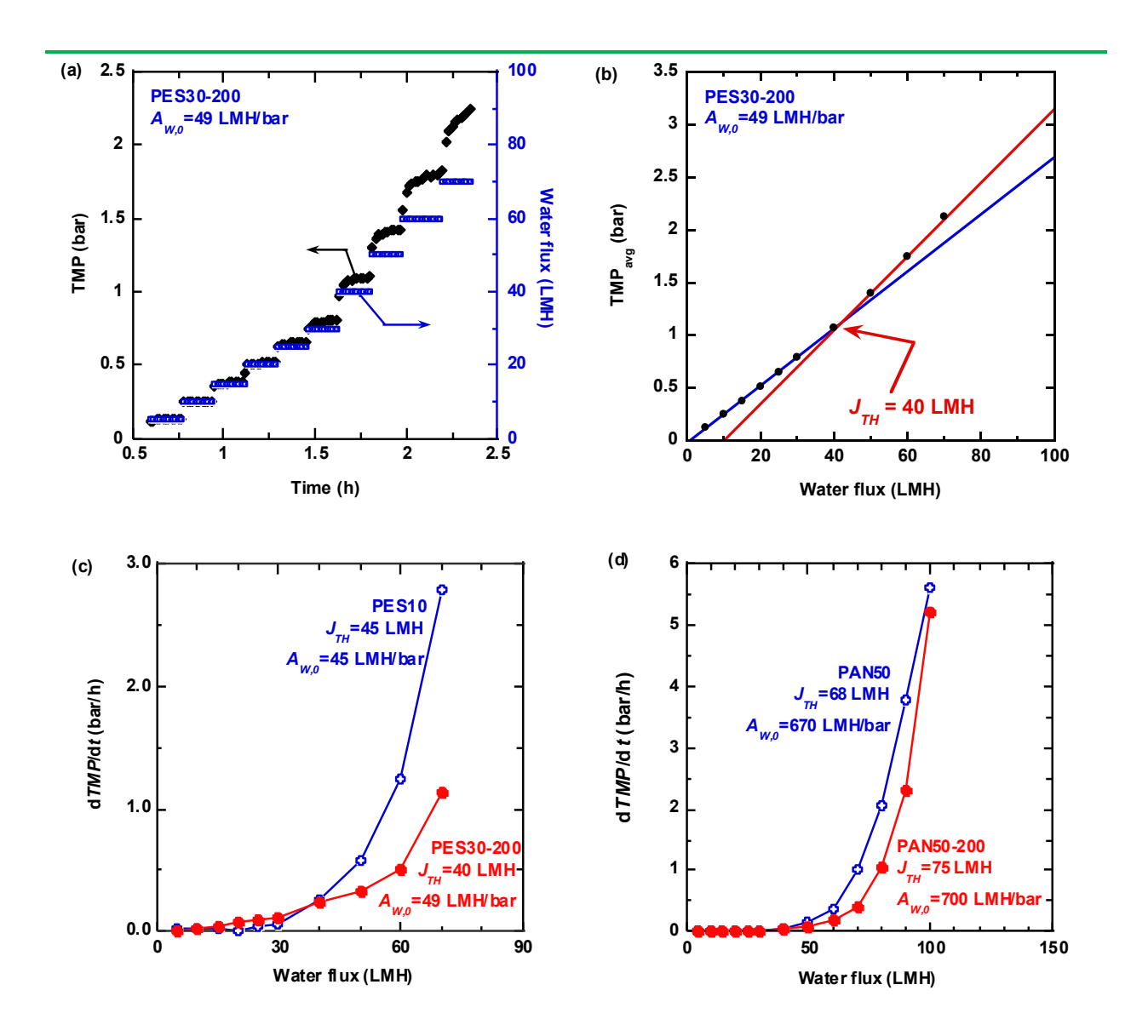


**Figure 5.** Antifouling properties of the fluorinated membranes determined using a constant-flux crossflow system. (a) TMP as a function of time and (b) the average TMP at each water flux for PES30-200. Comparison of the dTMP/dt at each water flux for (c) PES30 and PES30-200, and

(d) PAN50 and PAN50-200. The  $J_{TH}$  values were determined from the flux stepping experiments. The feed contains 0.5 g/L BSA at  $\approx$ 22 °C and has a Reynolds number of 1500 and a velocity of 0.38 m/s.

To elucidate the effect of surface fluorination on the antifouling properties, the fluorinated membranes should be compared with the pristine ones with similar water permeance and  $J_{TH}$  values. As PES30-200 has lower water permeance and  $J_{TH}$  than PES30, PES10 is chosen for comparison, which has slightly lower water permeance but higher  $J_{TH}$  (cf. Figures S3d and 5c) presumably because of the different pore sizes and distribution. Figure 5c compares the rate of the TMP increase over time (i.e., dTMP/dt) at each flux step for these two membranes. Larger dTMP/dt values indicate greater tendency for fouling in the membranes. At the water fluxes below their  $J_{TH}$  (40 LMH), both membranes show comparable fouling rates despite the lower  $J_{TH}$  value in PES30-200, while at the water fluxes above 40 LMH, the fluorinated membrane exhibits much lower values of dTMP/dt than PES-10. These results confirm the enhancement of the antifouling properties by the surface fluorination, though PES30-200 does not exhibit more superior antifouling properties than PES-10.

Figure 5d demonstrates the improved antifouling properties by surface fluorination of PAN UF membranes. PAN50 exhibits water permeance of 670 LMH/bar and  $J_{TH}$  value of 68 LMH, while PAN50-200 shows similar water permeance (700 LMH/bar) but higher  $J_{TH}$  value (75 LMH, cf. Figure S3). The slightly higher water permeance in the fluorinated membrane is caused by the variance of the membrane sample. On the other hand, this is very different from PES30 because PAN50 has larger surface pores than PES30, and the reduced pore size caused by the coating layer does not decrease water permeance as much as PES30-200. By contrast, PAN50-200 exhibits

higher  $J_{TH}$  value, validating the improved antifouling properties derived from the fluorination. More importantly, at the water flux of 60 LMH (lower than the  $J_{TH}$  values of both membranes), PAN50-200 shows the dTMP/dt value 54% lower than PAN50.

#### 4. CONCLUSIONS

We demonstrate facile fluorination of UF membrane surface by directly coating non-stick Teflon AF1600 to achieve superior antifouling properties while retaining high water permeance. This amorphous perfluoropolymer can be easily deposited on the solid portion of the membranes with different hydrophilicity (PES and PAN) without covering the pores (as shown by the SEM and MWCO measurement), leading to high water permeance. As the Teflon AF1600 concentration increases from 0 to 500 ppm, the coating layer thickness increases from 0 to 7.0 nm, and the BSA adsorption decreased from 11 µg/cm<sup>2</sup> to 2.5 µg/cm<sup>2</sup>. The surface energy of the fluorinated membranes is close to that for the minimal biological fouling as described in the Baier's curve. In dead-end filtration systems, the PES30-200 exhibits a 35% reduction in water permeance, less than the unmodified one (50% reduction) for obtaining the same amount of permeated water. In the constant-flux crossflow system, PAN50-200 shows water permeance similar to and J<sub>TH</sub> value higher than PAN50, and the fouling rate (as indicated by dTMP/dt) of PAN50-200 is only 46% that of the PAN50 at an operational water flux of 60 LMH. This facile surface fluorination can be easily integrated into the current membrane manufacturing processes, rendering its potential for practical applications.

#### ■ ASSOCIATED CONTENT

**Supporting Information (SI)** 

The SI is available free of charge via the Internet at http://pubs.acs.org.

Surface tension and SEM photos of the fluorinated membranes; schematic of the constant-flux

system; additional results of antifouling properties in the pristine and fluorinated membranes.

■ AUTHOR INFORMATION

**Corresponding Author** 

\*E-mail: haiqingl@buffalo.edu

**ORCID** 

Haiqing Lin: 0000-0001-8042-154X

**Author Contributions** 

The manuscript was prepared through the contributions of all authors. All authors have approved

the final version of the manuscript.

**Notes** 

The authors declare no competing financial interest.

■ ACKNOWLEDGMENTS

We acknowledge the financial support from the U.S. National Science Foundation (NSF Award

1635026).

**■ REFERENCES** 

Park, H. B.; Kamcev, J.; Robeson, L. M.; Elimelech, M.; Freeman, B. D., Maximizing the 1.

right stuff: The trade-off between membrane permeability and selectivity. Science 2017, 356

(6343), eaab0530.

21

- 2. Geise, G. M.; Paul, D. R.; Freeman, B. D., Fundamental water and salt transport properties of polymeric materials. *Prog. Polym. Sci.* **2014**, *39* (1), 1-24.
- 3. Werber, J. R.; Osuji, C. O.; Elimelech, M., Materials for next-generation desalination and water purification membranes. *Nat. Rev. Mater.* **2016**, *I* (5), 16018.
- 4. Miller, D.; Dreyer, D.; Bielawski, C.; Paul, D.; Freeman, B., Surface modification of water purification membranes: A review. *Angew. Chem. Int. Ed.* **2017**, *56* (17), 4662-4711.
- 5. Shahkaramipour, N.; Tran, T.; Ramanan, S.; Lin, H., Membranes with surface-enhanced antifouling properties for water purification. *Membranes* **2017**, *7* (1), 13.
- 6. Zhang, R.; Liu, Y.; He, M.; Su, Y.; Zhao, X.; Elimelech, M.; Jiang, Z., Antifouling membranes for sustainable water purification: Strategies and mechanisms. *Chem. Soc. Rev.* **2016**, *45* (21), 5888-5924.
- 7. Amin, I. N. H. M.; Mohammad, A. W.; Markom, M.; Peng, L. C.; Hilal, N., Flux decline study during ultrafiltration of glycerin-rich fatty acid solutions. *J. Membr. Sci.* **2010**, *351* (1-2), 75-86.
- 8. Ju, H.; McCloskey, B. D.; Sagle, A. C.; Kusuma, V. A.; Freeman, B. D., Preparation and characterization of crosslinked poly(ethylene glycol) diacrylate hydrogels as fouling-resistant membrane coating materials. *J. Membr. Sci.* **2009**, *330* (1-2), 180-188.
- 9. Miller, D. J.; Huang, X. F.; Li, H.; Kasemset, S.; Lee, A.; Agnihotri, D.; Hayes, T.; Paul, D. R.; Freeman, B. D., Fouling-resistant membranes for the treatment of flowback water from hydraulic shale fracturing: A pilot study. *J. Membr. Sci.* **2013**, *437*, 265-275.
- 10. Louie, J. S.; Pinnau, I.; Ciobanu, I.; Ishida, K. P.; Ng, A.; Reinhard, M., Effects of polyether-polyamide block copolymer coating on performance and fouling of reverse osmosis membranes. *J. Membr. Sci.* **2006**, *280* (1-2), 762-770.

- 11. McCloskey, B. D.; Park, H. B.; Ju, H.; Rowe, B. W.; Miller, D. J.; Freeman, B. D., A bioinspired fouling-resistant surface modification for water purification membranes. *J. Membr. Sci.* **2012**, *413*, 82-90.
- 12. Kirschner, A. Y.; Chang, C.-C.; Kasemset, S.; Emrick, T.; Freeman, B. D., Fouling-resistant ultrafiltration membranes prepared via co-deposition of dopamine/zwitterion composite coatings. *J. Membr. Sci.* **2017**, *541*, 300-311.
- 13. Chang, C. C.; Kolewe, K. W.; Li, Y.; Kosif, I.; Freeman, B. D.; Carter, K. R.; Schiffman,
- J. D.; Emrick, T., Underwater superoleophobic surfaces prepared from polymer zwitterion/dopamine composite coatings. *Adv. Mater. Interfaces* **2016**, *3* (6), 1500521.
- 14. Shahkaramipour, N.; Lai, C. K.; Venna, S. R.; Sun, H.; Cheng, C.; Lin, H., Membrane surface modification using thiol-containing zwitterionic polymers via bioadhesive polydopamine. *Ind. Eng. Chem. Res.* **2018**, *57* (6), 2336-2345.
- 15. Shahkaramipour, N.; Ramanan, S. N.; Fister, D.; Park, E.; Venna, S. R.; Sun, H.; Cheng, C.; Lin, H., Facile grafting of zwitterions onto the membrane surface to enhance antifouling properties for wastewater reuse. *Ind. Eng. Chem. Res.* **2017**, *56* (32), 9202-9212.
- 16. Zhang, C.; Ma, M.; Chen, T.; Zhang, H.; Hu, D.; Wu, B.; Ji, J.; Xu, Z., Dopamine-triggered one-step polymerization and codeposition of acrylate monomers for functional coatings. *ACS Appl. Mater. Inter.* **2017**, *9* (39), 34356-34366.
- 17. Aksoy, C.; Kaner, P.; Asatekin, A.; Culfaz-Emecen, P. Z., Co-deposition of stimuli-responsive microgels with foulants during ultrafiltration as a fouling removal strategy. *ACS Appl. Mater. Inter.* **2019**, *11* (20), 18711-18719.

- 18. Kaner, P.; Dudchenko, A. V.; Mauter, M. S.; Asatekin, A., Zwitterionic copolymer additive architecture affects membrane performance: fouling resistance and surface rearrangement in saline solutions. *J. Mater. Chem. A* **2019**, *7* (9), 4829-4846.
- 19. Nurioglu, A. G.; Esteves, A. C. C.; de With, G., Non-toxic, non-biocide-release antifouling coatings based on molecular structure design for marine applications. *J. Mater. Chem. B* **2015**, *3* (32), 6547-6570.
- 20. Lejars, M.; Margaillan, A.; Bressy, C., Fouling release coatings: A nontoxic alternative to biocidal antifouling coatings. *Chem. Rev.* **2012**, *112* (8), 4347-4390.
- 21. Li, Y.; Su, Y.; Zhao, X.; Zhang, R.; Zhao, J.; Fan, X.; Jiang, Z., Surface fluorination of polyamide nanofiltration membrane for enhanced antifouling property. *J. Membr. Sci.* **2014**, *455*, 15-23.
- 22. Ozaydin-Ince, G.; Matin, A.; Khan, Z.; Zaidi, S. M. J.; Gleason, K. K., Surface modification of reverse osmosis desalination membranes by thin-film coatings deposited by initiated chemical vapor deposition. *Thin Solid Films* **2013**, *539*, 181-187.
- 23. Zhao, X.; Su, Y.; Chen, W.; Peng, J.; Jiang, Z., Grafting perfluoroalkyl groups onto polyacrylonitrile membrane surface for improved fouling release property. *J. Membr. Sci.* **2012**, *415-416*, 824-834.
- 24. Anamelechi, C. C.; Truskey, G. A.; Reichert, W. M., Mylar and Teflon-AF as cell culture substrates for studying endothelial cell adhesion. *Biomaterials* **2005**, *26*, 6887-6896.
- 25. Yavari, M.; Le, T.; Lin, H., Physical aging of glassy perfluoropolymers in thin film composite membranes. Part I. Gas transport properties. *J. Membr. Sci.* **2017**, *525*, 387-398.

- 26. Zhu, L.; Yavari, M.; Jia, W.; Furlani, E. P.; Lin, H., Geometric restriction of gas permeance in ultrathin film composite membranes evaluated using an integrated experimental and modeling approach. *Ind. Eng. Chem. Res.* **2017**, *56* (1), 351–358.
- 27. Ebnesajjad, S., 3. Surface Energy of Solids. In *Surface Treatment of Materials for Adhesion Bonding*, William Andrew Publishing: pp 29-42.
- 28. Żenkiewicz, M., Methods for the calculation of surface free energy of solids. *J. Achiev. Mater. Manuf. Eng.* **2007,** *24* (1), 137-145.
- 29. Wang, C.; Brown, G. O.; Burris, D. L.; Korley, L. T. J.; Epps, T. H., Coating architects: Manipulating multiscale structures to optimize interfacial properties for coating applications. *ACS Appl. Polym. Sci.* **2019**, *1* (9), 2249-2266.
- 30. Xu, J. L.; Tran, T. N.; Lin, H.; Dai, N., Removal of disinfection byproducts in forward osmosis for wastewater recycling. *J. Membr. Sci.* **2018**, *564*, 352-360.
- 31. Tran, T. N.; Ramanan, S. N.; Lin, H., Synthesis of hydrogels with antifouling properties as membranes for water purification. *J. Vis. Exp.* **2017**, (122), e55426.
- 32. Zhao, S.; Huang, K.; Lin, H., Impregnated membranes for water purification using forward osmosis. *Ind. Eng. Chem. Res.* **2015**, *54* (49), 12354-12366.
- 33. Chen, W.; Peng, J.; Su, Y.; Zheng, L.; Wang, L.; Jiang, Z., Separation of oil/water emulsion using Pluronic F127 modified polyethersulfone ultrafiltration membranes. *Sep. Purif. Technol.* **2009**, *66* (3), 591-597.
- 34. Miller, D. J.; Paul, D. R.; Freeman, B. D., A crossflow filtration system for constant permeate flux membrane fouling characterization. *Rev. Sci. Instrum.* **2013**, *84* (3), 035003.
- 35. Baier, R. E., Surface behaviour of biomaterials: The theta surface for biocompatibility. *J. Mater. Sci.: Mater. Med.* **2006**, *17* (11), 1057.

- 36. Christopher, O., Fifty years of the Baier curve: progress in understanding antifouling coatings. *Green Mater.* **2017**, *5* (1), 1-3.
- 37. Nason, T. C.; Moore, J. A.; Lu, T. M., Deposition of amorphous fluoropolymer thin films by thermolysis of Teflon amorphous fluoropolymer. *Appl. Phys. Lett.* **1992**, *60*, 1866.
- 38. Epstein, A. K.; Wong, T.-S.; Belisle, R. A.; Boggs, E. M.; Aizenberg, J., Liquid-infused structured surfaces with exceptional anti-biofouling performance. *Proc. Natl. Acad. Sci. U.S.A.* **2012**, *109* (33), 13182.
- 39. Gudipati, C. S.; Finlay, J. A.; Callow, J. A.; Callow, M. E.; Wooley, K. L., The antifouling and fouling-release performance of hyperbranched fluoropolymer (HBFP)-poly(ethylene glycol) (PEG) composite coatings evaluated by adsorption of biomacromolecules and the green fouling alga Ulva. *Langmuir* **2005**, *21*, 3044–3053.
- 40. Miller, D. J.; Kasemset, S.; Paul, D. R.; Freeman, B. D., Comparison of membrane fouling at constant flux and constant transmembrane pressure conditions. *J. Membr. Sci.* **2014**, *454*, 505-515.
- 41. Field, R. W.; Pearce, G. K., Critical, sustainable and threshold fluxes for membrane filtration with water industry applications. *Adv. Colloid Interface Sci.* **2011**, *164* (1), 38-44.
- 42. Miller, D. J.; Kasemset, S.; Wang, L.; Paul, D. R.; Freeman, B. D., Constant flux crossflow filtration evaluation of surface-modified fouling-resistant membranes. *J. Membr. Sci.* **2014**, *452*, 171-183.
- 43. Beier, S. P.; Jonsson, G., Critical flux determination by flux-stepping. *AIChE J.* **2010**, *56* (7), 1739-1747.
- 44. Kirschner, A. Y.; Cheng, Y.-H.; Paul, D. R.; Field, R. W.; Freeman, B. D., Fouling mechanisms in constant flux crossflow ultrafiltration. *J. Membr. Sci.* **2019**, *574*, 65-75.

45. Kasemset, S.; He, Z.; Miller, D. J.; Freeman, B. D.; Sharma, M. M., Effect of polydopamine deposition conditions on polysulfone ultrafiltration membrane properties and threshold flux during oil/water emulsion filtration. *Polymer* **2016**, *97*, 247-257.